Quantum Fluctuations to Cause the Breakdown of the Spin-1 Haldane Phase

Shoji Yamamoto
Department of Physics, Faculty of Science, Okayama University,
Tsushima, Okayama 700, Japan
(Received)

Investigating quantum fluctuations in the ground states of $S = 1$ quantum antiferromagnetic spin chains described by the bilinear-biquadratic Hamiltonian $\mathcal{H} = \sum_i \left[S_i \cdot S_{i+1} + \beta (S_i \cdot S_{i+1})^2 \right]$, we study a mechanism of the breakdown of the Haldane phase. Based on the valence-bond-solid structure, but replacing two links of them by triplet bonds (*crackions*), we construct a trial wave function which is singlet and translationally invariant, where the crackion-crackion distance is regarded as a variational parameter. At $\beta < 1/3$, the minimization of the variational energy results in a bound state of crackions, while at $\beta > 1/3$, crackions come to be set free from their bound state with increase of β and the chain length. We point out that the breakdown of the Haldane phase with β approaching 1 can be attributed to the collapse of the bound state and the growth of a short-range repulsive interaction between crackions.

PACS numbers: 75.10.Jm, 75.50.Ee,75.60.Ch

I. INTRODUCTION

Since Haldane [1] proposed that the one-dimensional spin-S Heisenberg antiferromagnet should exhibit qualitatively different properties according to whether S is integer or half odd integer, low-temperature properties of integer-spin chains have been of great interest. Various numerical tools [2,3,4,5,6] brought us precise estimates of the excitation gap immediately above the ground state and visualized the Haldane massive phase. On the other hand, a rigorous treatment [7] performed by Affleck, Kennedy, Lieb, and Tasaki (AKLT) considerably contributed to understanding of the physical mechanism of this phenomenon. They considered a special bilinear-biquadratic Hamiltonian of $S = 1$,

$$\mathcal{H} = \sum_i \left[\boldsymbol{S}_i \cdot \boldsymbol{S}_{i+1} + \frac{1}{3} (\boldsymbol{S}_i \cdot \boldsymbol{S}_{i+1})^2 \right] , \tag{1.1}$$

and constructed its ground state using valence bonds, which they call a valence-bond-solid (VBS) state. This model possesses the unique disordered ground state with a finite gap to the excited states and therefore exhibits the typical nature peculiar to the Haldane phase. Keeping in mind that within a naive variational treatment [8,9,10,11,12] the ground states of a certain class of Hamiltonians are all approximated by the VBS state, we are convinced that the appearance of the Haldane phase is generally described in terms of the VBS picture.

The AKLT model reveals that there lies a hidden topological order [13,14] in the Haldane phase, which can be measured by the string order parameter of den Nijs and Rommelse [15],

$$O^z_{\rm string} = \lim_{|i-j| \to \infty} \langle S^z_i \prod_{k=i}^{j-1} \exp[{\rm i}\pi S^z_k] S^z_j \rangle , \tag{1.2}$$

where $\langle \ \ \rangle$ denotes the expectation value in the ground state. Since the string order parameter takes its full value 4/9 in the VBS state, any excitation of the VBS state should more or less reduce the hidden antiferromagnetic order. A local defect in the VBS state is obtained by replacing its arbitrary link by a triplet bond [16]. This spin-1 excitation, which is called a *crackion*, has a solitonic nature. Actually, a moving crackion and a moving domain wall in the hidden antiferromagnetic order both result in the same dispersion relation [17,18]. Furthermore, Scharf and Mikeska [19] reported that modified crackions, which they call dressed solitonic excitations, almost perfectly reproduce the low-lying excitations of the AKLT model [18]. Not only variational treatments [20,21,22] but also numerical investigations [2,23,24,25,26,27] showed that the idea of domain walls appearing in the hidden order well applies to the low-lying excitations of the Heisenberg Hamiltonian as well.

Thus the low-energy structure of $S = 1$ antiferromagnetic spin chains is well described by the VBS ground state and the solitonic excitations in its hidden topological order. However, we have, on the other hand, to recognize that once the Hamiltonian deviates from the AKLT point, quantum fluctuations begin to destroy the perfect hidden order. At the Heisenberg point, for example, $O^z_{\rm string}$ is reduced to 0.374 [2,12,27]. Although the VBS model elucidates the essential mechanism of the appearance of the Haldane phase, the breakdown of the Haldane phase is never understood without consideration of the quantum fluctuations. Since a density-matrix renormalization-group calculation [27] suggests that $O^z_{\rm string}$ persists as far as the system lies in the Haldane phase, the breakdown mechanism must be revealed in clarifying how the string order is reduced and disappears. Why is $O^z_{\rm string}$ able to remain finite in spite of fluctuations? What is the driving force of the collapse of the string order? In answering these questions, we have first to recognize that there exist two mechanisms to destroy the string order. One may be called the thermal

mechanism and explains how the string order vanishes at finite temperatures. The other may generically be called the quantum mechanism and explains how the ground-state phase transitions occur. The qualitative difference between them was pointed out by the present author and Miyashita [24]. Making use of quantum Monte Carlo snapshots, they demonstrated that thermal fluctuations can cause the collapse of the string order, whereas quantum fluctuations no more than reduce the string order (Fig. 1). It is worth mentioning that thermal and quantum fluctuations should be distinguished only in integer-spin chains. Figures 1(c) and 1(d) show that for $S = 1/2$ both thermal and quantum fluctuations merely result in a pair of domain walls in the antiferromagnetic order and therefore there is no qualitative difference between them. Thus we are well convinced that thermal fluctuations induced in the $S = 1$ Haldane phase indeed lead to the collapse of the string order. On the other hand, quantum Monte Carlo observations [24] of the ground state of the Heisenberg Hamiltonian suggest that there exists an attractive interaction between topological defects, which confines quantum fluctuations to producing local effects on the hidden order. Furthermore the present author [28] analytically demonstrated that quantum-machanically induced solitonic excitations are stabilized into a strongly bound state at the Heisenberg point. That is why the string order parameter persists, in spite of fluctuations, in the ground state of the $S = 1$ Heisenberg model.

Now we have to recognize that the quantum breakdown of the Haldane phase has remained unexplained. How does the bound state of the solitonic excitations behave as the Hamiltonian approaches critical points? This is the interest in this article. Because of two reasons, we take the $S = 1$ bilinear-biquadratic Hamiltonian

$$\mathcal{H} = \sum_{i=1}^{L} \left[\boldsymbol{S}_i \cdot \boldsymbol{S}_{i+1} + \beta (\boldsymbol{S}_i \cdot \boldsymbol{S}_{i+1})^2 \right] , \tag{1.3}$$

on a ring of L sites for our subject. First, the model contains the AKLT point, which allows us to make a variational approach at the idea of crackions appearing in the VBS background. Second, the model contains explicit critical points, which were revealed by the Bethe-ansatz method. One is the Uimin-Lai-Sutherland (ULS) point [29,30,31] of $\beta = 1$ and the the other is Takhtajan-Babujian (TB) point [32,33] of $\beta = -1$. Hence we can take advantage of the knowledge on the boundaries of the Haldane phase in investigating the mechanism of its breakdown. It is the growth of quantum fluctuations with β moving from 1/3 to 1 that we explicitly discuss here. Another boundary of the Haldane phase, $\beta = -1$, seems to be so far from the AKLT point as not to allow us to approach it with the same scenario as demonstrated in this article. We will briefly mention another possible scenario to destroy the string order in the final section.

Although quantum Monte Carlo snapshots are quite helpful in getting a qualitative view of fluctuations [24], they are not naively available in the region of $\beta > 0$ due to the negative-sign problem. Therefore, in order to investigate quantum fluctuations, we make an analytic approach constructing a physically-motivated trial wave function for the ground state. Here, we take little interest in obtaining a superior variational bound [10] on the ground-state energy but lay a great emphasis on clarifying how the pair-crackion fluctuations grow as β moves away from 1/3. The trial wave function is naive but interestingly suggests a probable mechanism for the breakdown of the Haldane phase caused by quantum fluctuations.

II. TRIAL WAVE FUNCTION

Before constructing a trial wave function, we briefly review our knowledge on the ground state of the model as a function of β. For recent years, the model has vigorously been argued and up to now turned out to exhibit at least three different phases:

- $-1 < \beta < 1$: Haldane phase [1,7] with a unique disordered ground state and a gapped spectrum.
- $\beta < -1$: Dimerized phase [34,35,36] with twofold degenerate ground states and a gapped spectrum.
- $1 < \beta$: Trimerized phase [8,37,38,39] with threefold degenerate ground states. Whether the spectrum is gapped or gapless has less been settled so far.

A qualitative description of the phase diagram is obtained by a simple variational treatment [8,10,38] employing three different balence-bond states,

$$|\mathrm{VBS}(L)\rangle = \mathrm{Tr}\left[g_1^s \otimes g_2^s \otimes \cdots \otimes g_L^s \right] , \tag{2.1a}$$
$$|\mathrm{Dimer}(L)\rangle = \mathrm{Tr}\left[f_1^s \otimes f_2^s \otimes \cdots \otimes f_L^s \right] , \tag{2.1b}$$
$$|\mathrm{Trimer}(L)\rangle = \mathrm{Tr}\left[h_1^s \otimes h_2^s \otimes \cdots \otimes h_L^s \right] , \tag{2.1c}$$

where

$$g_i^s = \begin{bmatrix} -|0\rangle_i & -\sqrt{2}|+\rangle_i \\ \sqrt{2}|-\rangle_i & |0\rangle_i \end{bmatrix} , \tag{2.2a}$$

$$f_{2i-1}^s = \begin{bmatrix} |-\rangle_{2i-1} & |0\rangle_{2i-1} & |+\rangle_{2i-1} \end{bmatrix} ,$$
$$f_{2i}^s = \mathrm{T} \begin{bmatrix} |+\rangle_{2i} & -|0\rangle_{2i} & |-\rangle_{2i} \end{bmatrix} , \tag{2.2b}$$

$$h_{3i-2}^s = \begin{bmatrix} \sqrt{2}|+\rangle_{3i-2} & |0\rangle_{3i-2} & \sqrt{2}|-\rangle_{3i-2} \end{bmatrix} ,$$
$$h_{3i-1}^s = \begin{bmatrix} 0 & \sqrt{2}|-\rangle_{3i-1} & -|0\rangle_{3i-1} \\ -\sqrt{2}|-\rangle_{3i-1} & 0 & \sqrt{2}|+\rangle_{3i-1} \\ |0\rangle_{3i-1} & -\sqrt{2}|+\rangle_{3i-1} & 0 \end{bmatrix} ,$$
$$h_{3i}^s = \mathrm{T} \begin{bmatrix} \sqrt{2}|+\rangle_{3i} & |0\rangle_{3i} & \sqrt{2}|-\rangle_{3i} \end{bmatrix} , \tag{2.2c}$$

with $|+\rangle_i$, $|0\rangle_i$, $|-\rangle_i$ being the S_i^z eigenstates for eigenvalues 1, 0, -1, respectively. $|\mathrm{VBS}(L)\rangle$ is the VBS state of AKLT type, which is homogeneous. $|\mathrm{Dimer}(L)\rangle$ and $|\mathrm{Trimer}(L)\rangle$ represent balence-bond states which are dimerized and trimerized, respectively. The linear combination of these three states,

$$|\Phi(L;\theta,\phi)\rangle = \cos\theta\,\frac{|\mathrm{VBS}(L)\rangle}{\|\mathrm{VBS}(L)\|} + \sin\theta\,\cos\phi\,\frac{|\mathrm{Dimer}(L)\rangle}{\|\mathrm{Dimer}(L)\|} + \sin\theta\,\sin\phi\,\frac{|\mathrm{Trimer}(L)\rangle}{\|\mathrm{Trimer}(L)\|}\,, \tag{2.3}$$

may be a naive but suggestive variational wave function for the ground state of the present Hamiltonian, where $\|A\|$ denotes the norm of the state vector $|A\rangle$. Because of the asymptotic orthogonality between the different balence-bond states, $|\Phi(L;\theta,\phi)\rangle$ is correctly normalized in the thermodynamic limit. The variational energy is obtained as

$$\lim_{L\to\infty}\frac{\langle\Phi(L;\theta,\phi)|\mathcal{H}|\Phi(L;\theta,\phi)\rangle}{L} = -\frac{4}{3} + 2\beta + \sin^2\theta\left[\frac{1}{3} + \frac{2}{3}\beta + \sin^2\phi\left(\frac{1}{3} - \frac{14}{9}\beta\right)\right]\,, \tag{2.4}$$

which leads to a simple solution,

$$\begin{array}{ll} \theta = \frac{\pi}{2}\,,\ \phi = 0 & (\beta < -\frac{1}{2})\,, \\ \theta = 0 & (-\frac{1}{2} < \beta < \frac{3}{4})\,, \\ \theta = \frac{\pi}{2}\,,\ \phi = \frac{\pi}{2} & (\frac{3}{4} < \beta)\,. \end{array} \tag{2.5}$$

Thus we expect that in a certain region around the AKLT point, the low-energy physics of the model may be described in terms of the VBS picture. Although the model encounters a commensurate-incommensurate crossover [27,40] at a certain positive value of β, the gapped spectrum and the string order parameter both persist in the whole region between the TB ($\beta = -1$) and the ULS ($\beta = 1$) points [27].

We propose an idea of recognizing the breakdown of the Haldane phase with β moving away from the AKLT point as the growth of quantum fluctuations in the hidden antiferromagnetic order. The crackion with its spin projection λ ($\lambda = +, 0, -$) is created at the bond between sites i and $i+1$ replacing g_i^s by g_i^λ [11], where

$$g^+ = \begin{bmatrix} \sqrt{2}|+\rangle & 0 \\ -|0\rangle & 0 \end{bmatrix}\,,\quad g^0 = \begin{bmatrix} -|0\rangle & \sqrt{2}|+\rangle \\ \sqrt{2}|-\rangle & -|0\rangle \end{bmatrix}\,,\quad g^- = \begin{bmatrix} 0 & -|0\rangle \\ 0 & \sqrt{2}|-\rangle \end{bmatrix}\,. \tag{2.6}$$

The site indices have been omitted in Eq. (2.6) for the sake of simplicity. In order to describe the ground state, we introduce a trial wave function of zero momentum with a pair of crackions,

$$|\Psi(L;l,\alpha)\rangle = \frac{1}{\sqrt{L}}\sum_{i=1}^{L}\left[\frac{|\Psi^{+-}_{i,i+l}(L)\rangle}{\|\Psi^{+-}_{i,i+l}(L)\|} + \frac{|\Psi^{-+}_{i,i+l}(L)\rangle}{\|\Psi^{-+}_{i,i+l}(L)\|} - \alpha\frac{|\Psi^{00}_{i,i+l}(L)\rangle}{\|\Psi^{00}_{i,i+l}(L)\|}\right]\,, \tag{2.7}$$

where

$$|\Psi^{\lambda\mu}_{i,i+l}(L)\rangle = \begin{cases} \mathrm{Tr}\left[g_1^s\otimes\cdots\otimes g_{i-1}^s\otimes g_i^\lambda\otimes g_{i+1}^s\otimes\cdots \right. \\ \qquad \left.\otimes g_{i+l-1}^s\otimes g_{i+l}^\mu\otimes g_{i+l+1}^s\otimes\cdots\otimes g_L^s\right] \\ \qquad\qquad \text{for } 1\le l\le L/2\,, \\ \mathrm{Tr}\left[g_1^s\otimes\cdots\otimes g_L^s\right] \qquad \text{for } l = 0\,. \end{cases} \tag{2.8}$$

Here, the crackion-crackion distance l is regarded as a variational parameter, whereas α has just been introduced so as to symmetrize the two crackions into a spin singlet. The condition of the total spin singlet,

$$\sum_{i,j=1}^{L}\langle\Psi(L;l,\alpha)|\boldsymbol{S}_i\cdot\boldsymbol{S}_j|\Psi(L;l,\alpha)\rangle = 0\,, \tag{2.9}$$

results in

$$\alpha = \alpha_0 \equiv \sqrt{\frac{3^L + 3(-1)^L}{3^L + (-1)^l 3^{L-l} + (-1)^{L-l}3^l + (-1)^L}}\,. \tag{2.10}$$

We note that α_0 generally deviates from unity. This is because a crackion has its internal structure and spreads over neighboring sites. It is convincing that α_0 coincides with unity only in the limit of $L\to\infty$ and $l(\le L/2)\to\infty$. On the other hand, the minimization of the variational energy with respect to α,

$$\frac{\partial}{\partial\alpha}\frac{\langle\Psi(L;l,\alpha)|\mathcal{H}|\Psi(L;l,\alpha)\rangle}{\langle\Psi(L;l,\alpha)|\Psi(L;l,\alpha)\rangle} = 0\,, \tag{2.11}$$

also results in Eq. (2.10). In this sense the trial wave function employed is reasonable enough to investigate the ground-state fluctuations of the present Hamiltonian.

Hereafter we fix α to α_0 and calculate the variational energy as a function of L, l, and β,

$$E(L;l,\beta) \equiv \frac{\langle\Psi(L;l,\alpha_0)|\mathcal{H}|\Psi(L;l,\alpha_0)\rangle}{\langle\Psi(L;l,\alpha_0)|\Psi(L;l,\alpha_0)\rangle}\,. \tag{2.12}$$

The stabilization of the two-crackion state is measured by the energy difference

$$\Delta E(L;l,\beta) \equiv E(L;l,\beta) - E(L;0,\beta)\,. \tag{2.13}$$

The variational energy (2.12) is constructed from the quantum averages $\langle\Psi^{\lambda\mu}_{i,i+l}(L)|\boldsymbol{S}_m\cdot\boldsymbol{S}_{m+1}|\Psi^{\kappa\nu}_{j,j+l}(L)\rangle$ and $\langle\Psi^{\lambda\mu}_{i,i+l}(L)|(\boldsymbol{S}_m\cdot\boldsymbol{S}_{m+1})^2|\Psi^{\kappa\nu}_{j,j+l}(L)\rangle$, which are represented in the form of matrix-product type and therefore calculated by the use of the transfer-matrix technique [28,41,42,43]. The calculation is straightforward but exhausting due to plenty of indices appearing in the matrix elements. The explicit form of the variational energy is too lengthy to be presented even though α is fixed.

III. RESULTS

First, let us concentrate our attention on the Heisenberg point $\beta = 0$. We list in Table I the stabilization energy of the two-crackion state, $\Delta E(L; l, 0)$. With $\Delta E(L; l, 0) < 0$, a pair of crackions with their distance l may spontaneously occur in a chain of length L. The crackion fluctuation is even unstable in too short chains. Actually, at $L < 8$, the VBS state itself turns out to be the variational bound. However, a pair of crackions come to be stabilized into a strongly bound state with increase of L. The extremely small energy stabilization at $l = 1$ may be attributed to the fact that a crackion spreads over two sites. As L increases, the crackion pairs with larger values of l are stabilized one after another. However, the maximum distance between crackions keeping their formation energy negative stays four at $L = 1000$ and five even at $L = 10000$. Therefore two crackions can hardly move away from each other. Regarding L, as well as l, as a variational parameter, we obtain the variational bound on the ground-state energy per site, -1.37012987, at $L = 56$ and $l = 2$. Further increase of the chain length only reduces the crackion effect and ends in no stabilization of the ground state:

$$\lim_{L\to\infty} \frac{E(L;l)}{L} = \lim_{L\to\infty} \frac{\langle \mathrm{VBS}(L)|\mathcal{H}|\mathrm{VBS}(L)\rangle}{L\langle \mathrm{VBS}(L)|\mathrm{VBS}(L)\rangle} = -\frac{4}{3}\,. \quad (3.1)$$

The ground state in the long-chain limit should be described by a variational wave function with a finite crackion density. Alternatively, within an approximation neglecting the interaction between the bound crackion pairs, we may conclude that the best density of the crackion pairs is about 1/56. Thus we are led to a likely ground-state picture that pairs of crackions with $l \simeq 2$ appear in the VBS background keeping their density about 1/56. The true ground state is supposed to fluctuate around this picture. In fact the present variational bound has not yet reached the correct value $-1.402(1)$, which is a quantum Monte Carlo estimate of the per-site ground-state energy at $L = 56$. The rest of the correlation may be attributed to a spatial extension of a crackion, a breathing motion of two crackions within a pair, and an interaction between crackion pairs. A crackion is not equivalent to a hidden domain wall but indeed possesses a solitonic nature [18]. For example, there is a relation between a pair of hidden domain walls and crackion pairs:

$$S_i^{\pm} S_{i+l}^{\mp} |\mathrm{VBS}(L)\rangle = -|\Psi_{i-1,i+l-1}^{\pm\mp}(L)\rangle + |\Psi_{i-1,i+l}^{\pm\mp}(L)\rangle + |\Psi_{i,i+l-1}^{\pm\mp}(L)\rangle - |\Psi_{i,i+l}^{\pm\mp}(L)\rangle\,, \quad (3.2)$$

where we assume that $l \geq 2$. Considering that spin flips in pairs keeping the total magnetization constant do not necessarily cause a soliton-antisoliton pair in the hidden order (Fig. 2), the present variational calculation is well consistent with a direct observation of the ground state (Fig. 3).

Next, let us turn on the biquadratic interaction between neighboring spins. We plot in Fig. 4 the stabilization energy of the two-crackion state, $\Delta E(L; l, \beta)$, as a function of l changing L and β. The singularity observed around $L = l/2$ should be attributed to the periodic boundary condition. We find that the bound state of crackions, which is fully stabilized at the Heisenberg point, becomes less stable with increase of β. It is a matter of course that any crackion fluctuation causes an increase of the energy at the AKLT point $\beta = 1/3$, where the VBS state with the perfect hidden order is the exact ground state. Interestingly, in long enough chains at $\beta > 1/3$, a pair of crackions are less stable in a bound state than when they are far away from each other. As β moves away from 1/3 toward 1 as well as with increase of L, the attractive interaction between crackions changes into a repulsive one at small values of l. Although the stabilization energy per site is more and more reduced as L increases due to the reduction of the crackion density, yet the biquadratic interaction indeed turns the formation energy of well-separated two crackions negative in long enough chains. Hence a pair of crackions are set free from their bound state and are stabilized in their wide-range breathing motion with large enough values of β in long enough chains, as is illustrated in Fig. 5. We have already stated that the strong attractive interaction between crackions could allow the string order parameter to remain finite against quantum fluctuations. The collapse of the bound state of crackions and the growth of the short-range repulsive interaction between crackions, this is a probable mechanism of the quantum mechanical breakdown of the Haldane phase.

IV. SUMMARY AND DISCUSSION

We have investigated quantum fluctuations in the ground state of the spin-1 chain with the bilinear-biquadratic Hamiltonian. With the help of quantum Monte Carlo observations of the ground state, we have constructed a trial wave function with a pair of crackions appearing in the VBS background. We have demonstrated that two crackions are indeed stabilized into a strongly bound state at the Heisenberg point. While Monte Carlo snapshots are not available in the region of $\beta > 0$ due to the negative-sign problem, we have analytically revealed the scenario for the quantum mechanical collapse of the string order with β approaching 1. The disappearance of the attractive interaction sets crackions free from their bound state and the growth of a repulsive interaction causes crackions to move away from each other.

Besides the biquadratic interaction, there are many other factors to cause the breakdown of the Haldane

phase, such as an alternating or anisotropic interaction [11,12,44,45,46,47,48]. Therefore there may be any other scenario for quantum phase transitions. Actually we can not describe the Haldane-to-dimer phase transition with β approaching -1 by the same scenario. As β moves from $1/3$ to -1, the bound state of crackions remains fully stabilized. The TB point $\beta = -1$ might be too far from the AKLT point $\beta = 1/3$ to be discussed sharing the same physics with the VBS Hamiltonian. However, the picture of crackion pairs moving in the VBS background is still totally valid at the Heisenberg point [20,24]. Even though two crackions are stabilized into a bound state, bound crackion pairs with a high enough density can cause the collapse of the string order. The breakdown mechanism of the Haldane phase with β approaching -1 may be beyond the present approximation neglecting any interaction between crackion pairs. Since it is hardly feasible to perform a direct calculation of numbers of crackions keeping a definite picture of fluctuations, we expect alternative approaches [10,20] in the region of $\beta < 0$. Compared with the thermal breakdown, quantum phase transitions are various and complicated. We hope the present argument will motivate further study on the quantum mechanical breakdown of the Haldane phase.

ACKNOWLEDGMENTS

The author would like to thank K. Nomura for his helpful comments. A part of the numerical calculation was done using the facility of the supercomputer center, Institute for Solid State Physics, University of Tokyo. This work is supported in part by the Japanese Ministry of Education, Science, and Culture through the Grants-in-Aid (08740279, 09740286) and by the Okayama Foundation for Science and Technology.

[1] F. D. M. Haldane, Phys. Lett. **93A**, 464 (1983); Phys. Rev. Lett. **50**, 1153 (1983).
[2] S. R. White and D. A. Huse, Phys. Rev. B **48**, 3844 (1993).
[3] E. S. Sørensen and I. Affleck, Phys. Rev. Lett. **71**, 1633 (1993).
[4] O. Golinelli, Th. Jolicœur, and R. Lacaze, Phys. Rev. B **50**, 3037 (1994).
[5] U. Schollwöck and Th. Jolicœur, Europhys. Lett. **30**, 493 (1995).
[6] S. Yamamoto, Phys. Lett. A **213**, 102 (1996).
[7] I. Affleck, T. Kennedy, E. H. Lieb, and H. Tasaki, Phys. Rev. Lett. **59**, 799 (1987); Commun. Math. Phys. **115**, 477 (1988).
[8] K. Nomura and S. Takada, J. Phys. Soc. Jpn. **60**, 389 (1991).
[9] T. Kennedy and H. Tasaki, Commun. Math. Phys. **147**, 431 (1992).
[10] A. Schadschneider and J. Zittartz, Ann. Physik. **4**, 157 (1995).
[11] K. Totsuka, Y. Nishiyama, N. Hatano, and M. Suzuki, J. Phys.: Condens. Matter **7**, 4895 (1995).
[12] S. Yamamoto, Phys. Rev. B **55**, 3603 (1997).
[13] S. M. Girvin and D. P. Arovas, Phys. Scr. T **27**, 156 (1989).
[14] H. Tasaki, Phys. Rev. Lett. **66**, 798 (1991).
[15] M. den Nijs and K. Rommelse, Phys. Rev. B **40**, 4709 (1989).
[16] S. Knabe, J. Stat. Phys. **52**, 627 (1988).
[17] D. P. Arovas, A. Auerbach, and F. D. M. Haldane, Phys. Rev. Lett. **60**, 531 (1988).
[18] G. Fáth and J. Sólyom, J. Phys.: Condens. Matter **5**, 8983 (1993).
[19] R. Scharf and H.-J. Mikeska, J. Phys.: Condens. Matter **7**, 5083 (1995).
[20] G. Gómez-Santos, Phys. Rev. Lett. **63**, 790 (1989).
[21] H. Köhler and R. Schilling, J. Phys.: Condens. Matter **4**, 7899 (1992).
[22] U. Neugebauer and H.-J. Mikeska, Z. Phys. B **99**, 151 (1996).
[23] M. Takahashi, Phys. Rev. Lett. **62**, 2313 (1989).
[24] S. Yamamoto and S. Miyashita, Phys. Rev. B **48**, 9528 (1993).
[25] M. Takahashi, Phys. Rev. B **50**, 3045 (1994).
[26] S. Yamamoto and S. Miyashita, J. Phys. Soc. Jpn. **63**, 2866 (1994); to be published in Phys. Lett. A (1997).
[27] U. Schollwöck and Th. Jolicœur, and T. Garel, Phys. Rev. B **53**, 3304 (1996).
[28] S. Yamamoto, Phys. Lett. A **225**, 157 (1997).
[29] G. V. Uimi, JETP Lett. **12**, 225 (1970).
[30] C. K. Lai, J. Math. Phys. **15**, 1675 (1974).
[31] B. Sutherland, Phys. Rev. B **12**, 3795 (1975).
[32] L. A. Takhtajan, Phys. Lett. A **87**, 479 (1982).
[33] H. M. Babujian, Phys. Lett. A **90**, 479 (1982).
[34] J. Sólyom, Phys. Rev. B **36**, 8642 (1987).
[35] A. V. Chubukov, Phys. Rev. B **43**, 3337 (1991).
[36] Y. Xian, Phys. Lett. A **183**, 437 (1993).
[37] G. Fáth and J. Sólyom, Phys. Rev. B **44**, 11836 (1991); **47**, 872 (1993).
[38] Y. Xian, J. Phys.: Condens. Matter **5**, 7489 (1993).
[39] P. Reed, J. Phys.: Math. Gen. **27**, L69 (1994).
[40] R. J. Bursill, T. Xiang, G. A. Gehring, J. Phys.: Math. Gen. **28**, 2109 (1995).
[41] K. Totsuka and M. Suzuki, J. Phys.: Condens. Matter **7**, 1639 (1995).
[42] A. Klümper, A. Schadschneider, and J. Zittartz, J. Phys.: Math. Gen. **24**, L955 (1991).
[43] A. K. Kolezhuk, H.-J. Mikeska, and S. Yamamoto, Phys. Rev. B **55**, 3336 (1997).
[44] R. Botet and R. Julien, Phys. Rev. B **27**, 613 (1983); R. Botet, R. Julien, and M. Kolb, *ibid.* **28**, 3914 (1983).
[45] I. Affleck, Nucl. Phys. B **257**, 397 (1985); *ibid.* **265**, 409 (1986).
[46] R. R. P. Singh and M. P. Gelfand, Phys. Rev. Lett. **61**, 2133 (1988).
[47] Y. Kato and A. Tanaka, J. Phys. Soc. Jpn. **63**, 4327 (1994).
[48] S. Yamamoto, J. Phys. Soc. Jpn. **63**, 4327 (1994); Phys.

Rev. B **51**, 16128 (1995); *ibid.* **52**, 10170 (1995).
[49] A. Kitazawa, K. Nomura, and K. Okamoto, Phys. Rev. Lett. **76**, 4038 (1996).

FIG. 1. Typical fluctuations of the spin configuration. The black triangle denotes a domain wall in the (hidden) antiferromagnetic order. (a) A thermal fluctuation in the $S = 1$ system, which allows the total magnetization to change and therefore leads to the collapse of the long-range hidden antiferromagnetic order. (b) A quantum fluctuation in the $S = 1$ system, which keeps the total magnetization constant and therefore only produces a local effect on the hidden antiferromagnetic order. (c) A thermal fluctuation in the $S = 1/2$ system, which is, in contrast with the $S = 1$ case, nothing more than a local effect on the antiferromagnetic order. (d) A quantum fluctuation in the $S = 1/2$ system, which locally disturbs the antiferromagnetic order.

FIG. 2. Quantum fluctuations in the $S = 1$ ground state, where the total magnetization is kept constant and therefore spins flip in pairs. The black triangle denotes a domain wall in the hidden antiferromagnetic order. In the case (a), a soliton-antisoliton pair appears in the hidden order, whereas in the case (b), there appears no defect in the hidden order.

FIG. 3. A quantum Monte Carlo snapshot of the transformed two-dimensional Ising system of $L = 100$ at the $S = 1$ Heisenberg point under the temperature $k_{\rm B}T = 0.02$, where the horizontal and the vertical axes denote the chain and the Trotter directions corresponding to space and time, respectively. The temperature taken is low enough to represent the ground-state properties. We have set the Trotter number n equal to 48 and show the passage of time corresponding to $1/4k_{\rm B}T$. We encircle the antiphase domains which have the hidden antiferromagnetic order opposite to the background. The location of the domain walls is specified inevitably with some uncertainty owing to the liquid-like nature of the VBS state.

FIG. 4. The stabilization energy of the two-crackion state as a function of the crackion-crackion distance l at various values of the chain length L and the biquadratic interaction β, $\Delta E(L; l, \beta) \equiv E(L; l, \beta) - E(L; 0, \beta)$. (a) $L = 80$, (b) $L = 160$, (c) $L = 240$, (d) $L = 320$.

FIG. 5. Schematic representation of the ground-state spin configurations at distinct regions of the biquadratic interaction β. The black triangle denotes a domain wall in the hidden antiferromagnetic order. (a) The AKLT point $\beta = 1/3$. We observe a perfect hidden antiferromagnetic order. (b) $\beta < 1/3$. The domain walls are stabilized into a bound pair. The hidden antiferromagnetic order is reduced but still persists. (c) $\beta > 1/3$. The domain walls are set free from their bound state. The hidden antiferromagnetic order is nonlocally broken.

TABLE I. The stabilization energy of the two-crackion state as a function of the crackion-crackion distance l and the chain length L at the Heisenberg point, $\Delta E(L;l,0) \equiv E(L;l,0) - E(L;0,0)$.

l	$L=20$	$L=40$	$L=60$	$L=80$	$L=100$	$L=120$	$L=140$	$L=160$	$L=180$	$L=200$
1	-0.00000	-0.00000	-0.00000	-0.00000	-0.00000	-0.00000	-0.00000	-0.00000	-0.00000	-0.00000
2	0.20512	-1.33333	-2.20290	-2.76190	-3.15152	-3.43860	-3.65891	-3.83333	-3.97484	-4.09195
3	2.21638	1.43089	0.73563	0.11594	-0.43986	-0.94118	-1.39564	-1.80952	-2.18803	-2.53552
4	2.57370	2.44126	2.31010	2.18079	2.05330	1.92758	1.80360	1.68132	1.56071	1.44173
5	2.72694	2.71098	2.69141	2.67187	2.65236	2.63289	2.61345	2.59403	2.57465	2.55530
6	2.67604	2.69500	2.69236	2.68971	2.68706	2.68441	2.68177	2.67912	2.67648	2.67383
7	2.60728	2.71581	2.71546	2.71511	2.71476	2.71441	2.71407	2.71372	2.71337	2.71302
8	2.28123	2.70902	2.70898	2.70893	2.70889	2.70884	2.70880	2.70875	2.70871	2.70866
l	$L=220$	$L=240$	$L=260$	$L=280$	$L=300$	$L=320$	$L=340$	$L=360$	$L=380$	$L=400$
1	-0.00000	-0.00000	-0.00000	-0.00000	-0.00000	-0.00000	-0.00000	-0.00000	-0.00000	-0.00000
2	-4.19048	-4.27451	-4.34703	-4.41026	-4.46586	-4.51515	-4.55914	-4.59864	-4.63430	-4.66667
3	-2.85564	-3.15152	-3.42579	-3.68075	-3.91837	-4.14035	-4.34820	-4.54321	-4.72655	-4.89922
4	1.32436	1.20856	1.09429	0.98153	0.87025	0.76042	0.65201	0.54499	0.43934	0.33503
5	2.53599	2.51670	2.49744	2.47822	2.45903	2.43986	2.42073	2.40163	2.38256	2.36352
6	2.67119	2.66854	2.66590	2.66325	2.66061	2.65797	2.65533	2.65269	2.65005	2.64740
7	2.71267	2.71232	2.71197	2.71163	2.71128	2.71093	2.71058	2.71023	2.70988	2.70954
8	2.70862	2.70858	2.70853	2.70849	2.70844	2.70840	2.70835	2.70831	2.70826	2.70822
l	$L=420$	$L=440$	$L=460$	$L=480$	$L=500$	$L=520$	$L=540$	$L=560$	$L=580$	$L=600$
1	-0.00000	-0.00000	-0.00000	-0.00000	-0.00000	-0.00000	-0.00000	-0.00000	-0.00000	-0.00000
2	-4.69617	-4.72316	-4.74797	-4.77083	-4.79198	-4.81159	-4.82984	-4.84685	-4.86275	-4.87764
3	-5.06215	-5.21612	-5.36185	-5.50000	-5.63113	-5.75578	-5.87440	-5.98742	-6.09524	-6.19820
4	0.23203	0.13033	0.02989	-0.06931	-0.16728	-0.26406	-0.35966	-0.45411	-0.54742	-0.63962
5	2.34451	2.32553	2.30658	2.28767	2.26878	2.24992	2.23109	2.21230	2.19353	2.17479
6	2.64477	2.64213	2.63949	2.63685	2.63421	2.63157	2.62894	2.62630	2.62366	2.62103
7	2.70919	2.70884	2.70849	2.70814	2.70779	2.70745	2.70710	2.70675	2.70640	2.70605
8	2.70817	2.70813	2.70808	2.70804	2.70799	2.70795	2.70791	2.70786	2.70782	2.70777
l	$L=620$	$L=640$	$L=660$	$L=680$	$L=700$	$L=720$	$L=740$	$L=760$	$L=780$	$L=800$
1	-0.00000	-0.00000	-0.00000	-0.00000	-0.00000	-0.00000	-0.00000	-0.00000	-0.00000	-0.00000
2	-4.89162	-4.90476	-4.91715	-4.92884	-4.93989	-4.95035	-4.96028	-4.96970	-4.97865	-4.98718
3	-6.29662	-6.39080	-6.48101	-6.56749	-6.65047	-6.73016	-6.80674	-6.88041	-6.95131	-7.01961
4	-0.73072	-0.82075	-0.90973	-0.99767	-1.08459	-1.17051	-1.25544	-1.33941	-1.42242	-1.50450
5	2.15608	2.13740	2.11876	2.10014	2.08155	2.06299	2.04446	2.02596	2.00749	1.98904
6	2.61839	2.61576	2.61312	2.61049	2.60786	2.60522	2.60259	2.59996	2.59733	2.59470
7	2.70570	2.70536	2.70501	2.70466	2.70431	2.70396	2.70361	2.70327	2.70292	2.70257
8	2.70773	2.70768	2.70764	2.70759	2.70755	2.70750	2.70746	2.70741	2.70737	2.70733
l	$L=820$	$L=840$	$L=860$	$L=880$	$L=900$	$L=920$	$L=940$	$L=960$	$L=980$	$L=1000$
1	-0.00000	-0.00000	-0.00000	-0.00000	-0.00000	-0.00000	-0.00000	-0.00000	-0.00000	-0.00000
2	-4.99531	-5.00306	-5.01046	-5.01754	-5.02432	-5.03081	-5.03704	-5.04301	-5.04875	-5.05426
3	-7.08544	-7.14894	-7.21022	-7.26941	-7.32660	-7.38190	-7.43540	-7.48718	-7.53733	-7.58592
4	-1.58567	-1.66592	-1.74529	-1.82379	-1.90142	-1.97821	-2.05417	-2.12931	-2.20364	-2.27719
5	1.97063	1.95225	1.93389	1.91556	1.89727	1.87900	1.86076	1.84255	1.82436	1.80621
6	2.59207	2.58944	2.58681	2.58418	2.58155	2.57892	2.57629	2.57367	2.57104	2.56841
7	2.70222	2.70187	2.70152	2.70118	2.70083	2.70048	2.70013	2.69978	2.69944	2.69909
8	2.70728	2.70724	2.70719	2.70715	2.70710	2.70706	2.70701	2.70697	2.70692	2.70688

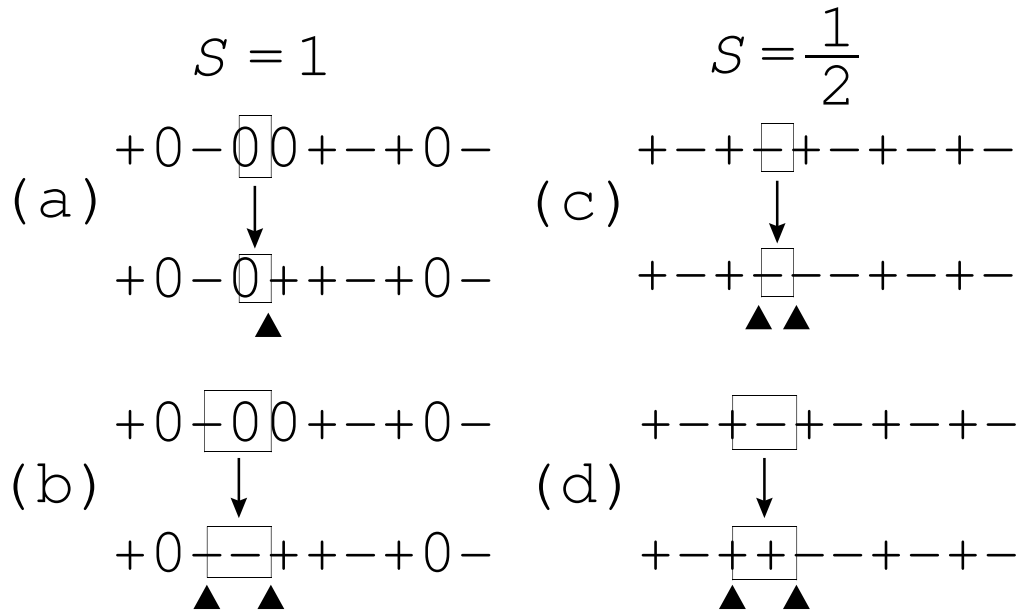

Fig.1

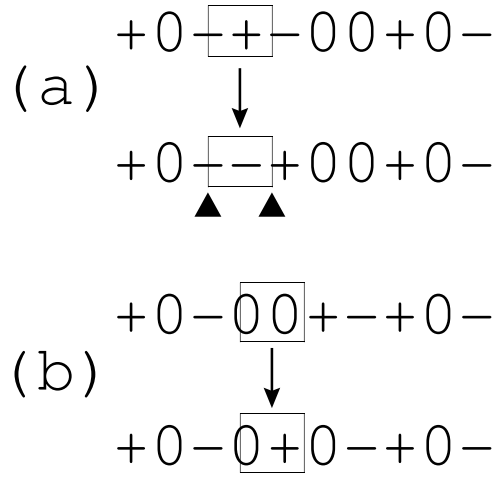

Fig.2

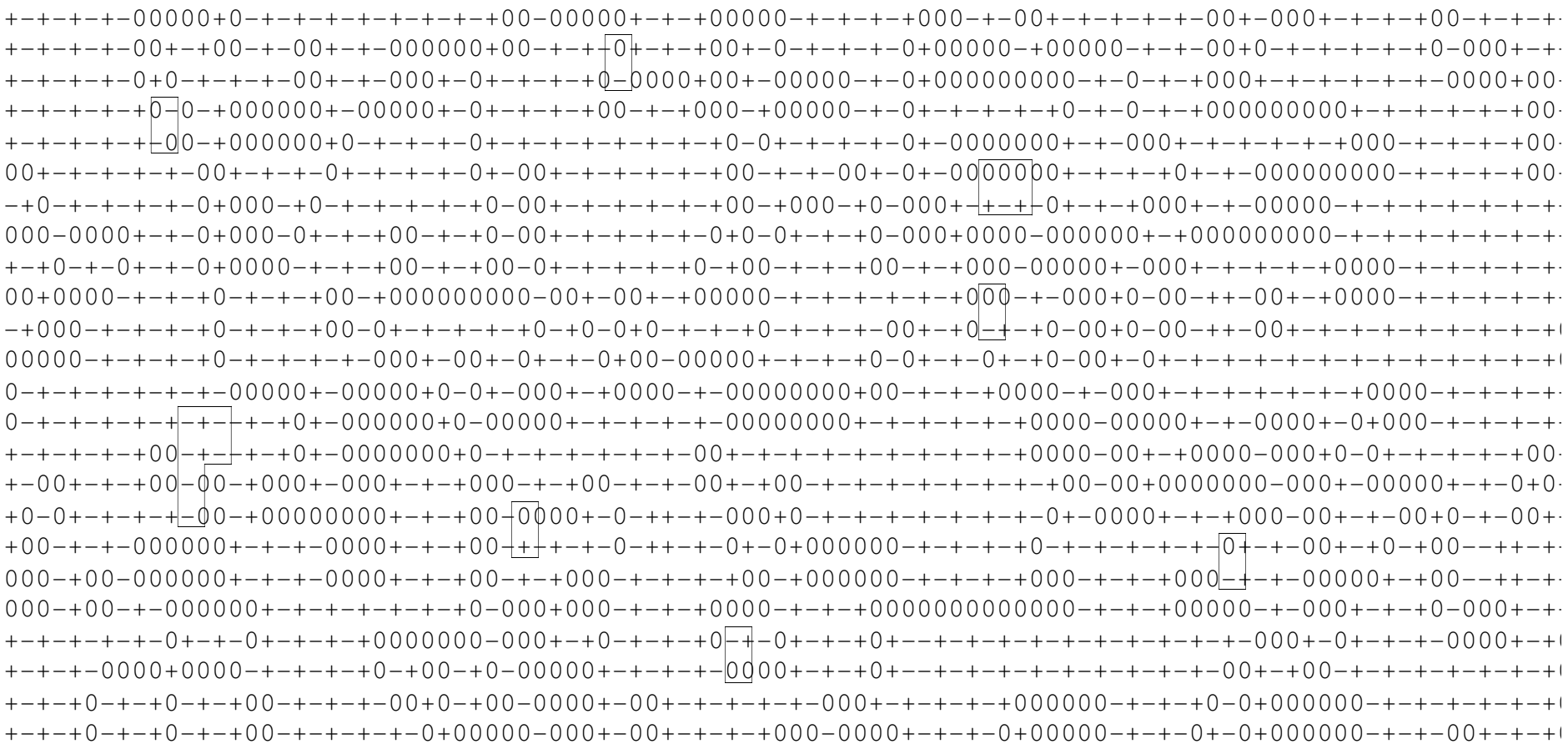

Fig.3

Fig.4(a)

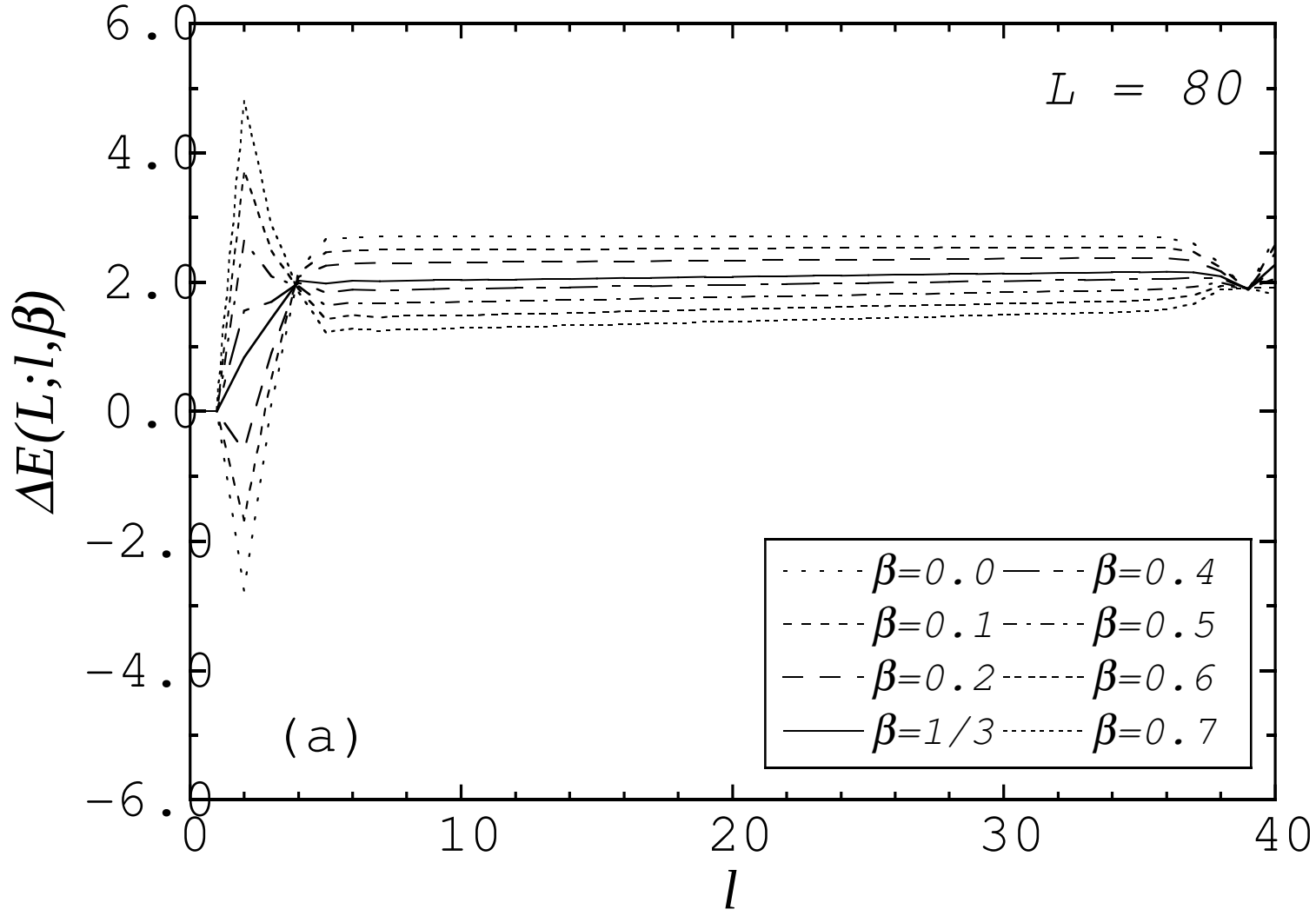
6.0
4.0
2.0
0.0
−2.0
−4.0
−6.0
0
10
20
30
40
l
ΔE(L;l,β)
L = 80
(a)
β=0.0
β=0.1
β=0.2
β=1/3
β=0.4
β=0.5
β=0.6
β=0.7

Fig.4(b)

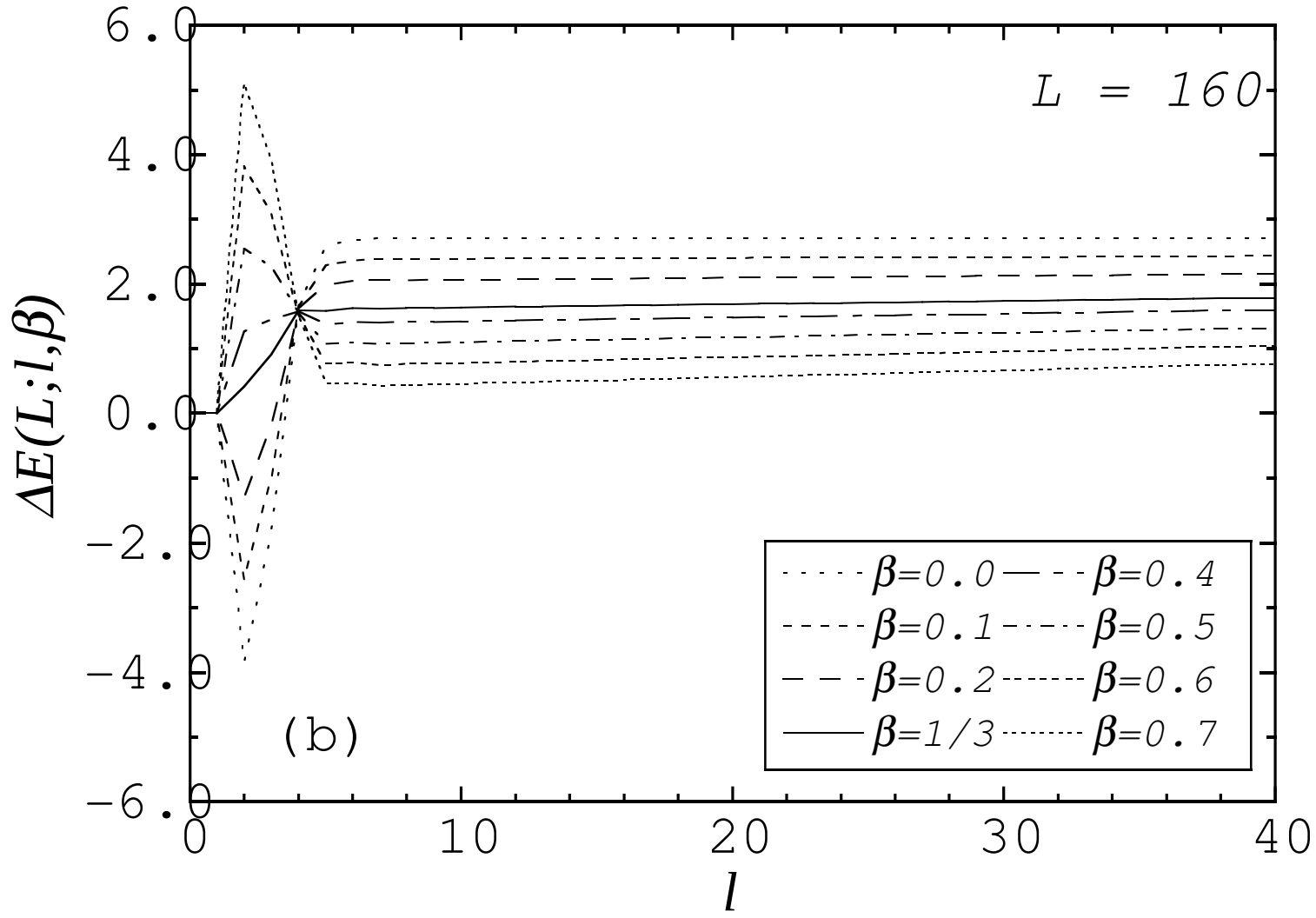
6.0
4.0
2.0
0.0
−2.0
−4.0
−6.0
0
10
20
30
40
l
ΔE(L;l,β)
L = 160
(b)
β=0.0
β=0.1
β=0.2
β=1/3
β=0.4
β=0.5
β=0.6
β=0.7

Fig.4(c)

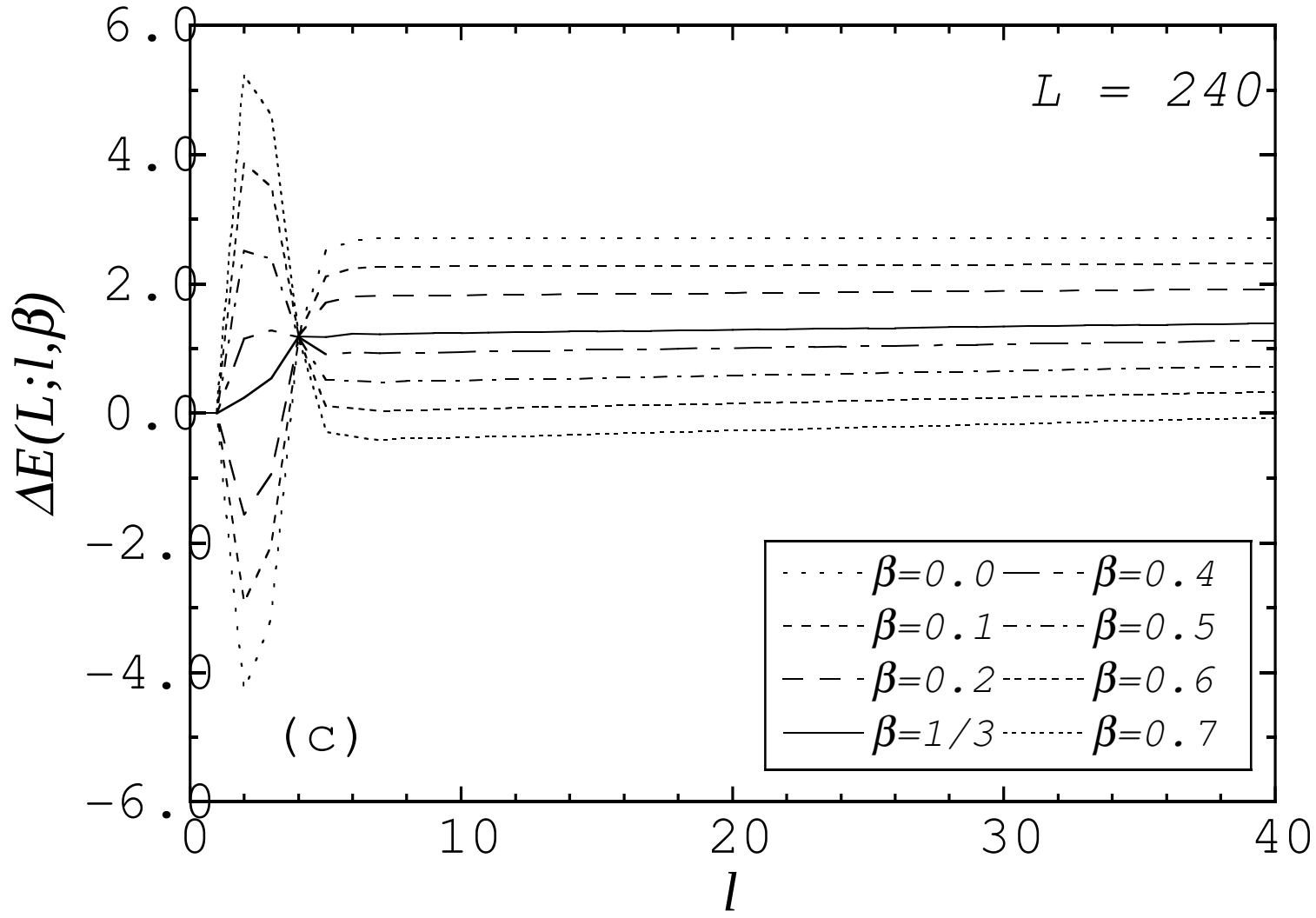
6.0
4.0
2.0
0.0
−2.0
−4.0
−6.0
0
10
20
30
40
l
ΔE(L;l,β)
L = 240
(c)
β=0.0
β=0.1
β=0.2
β=1/3
β=0.4
β=0.5
β=0.6
β=0.7

Fig.4(d)

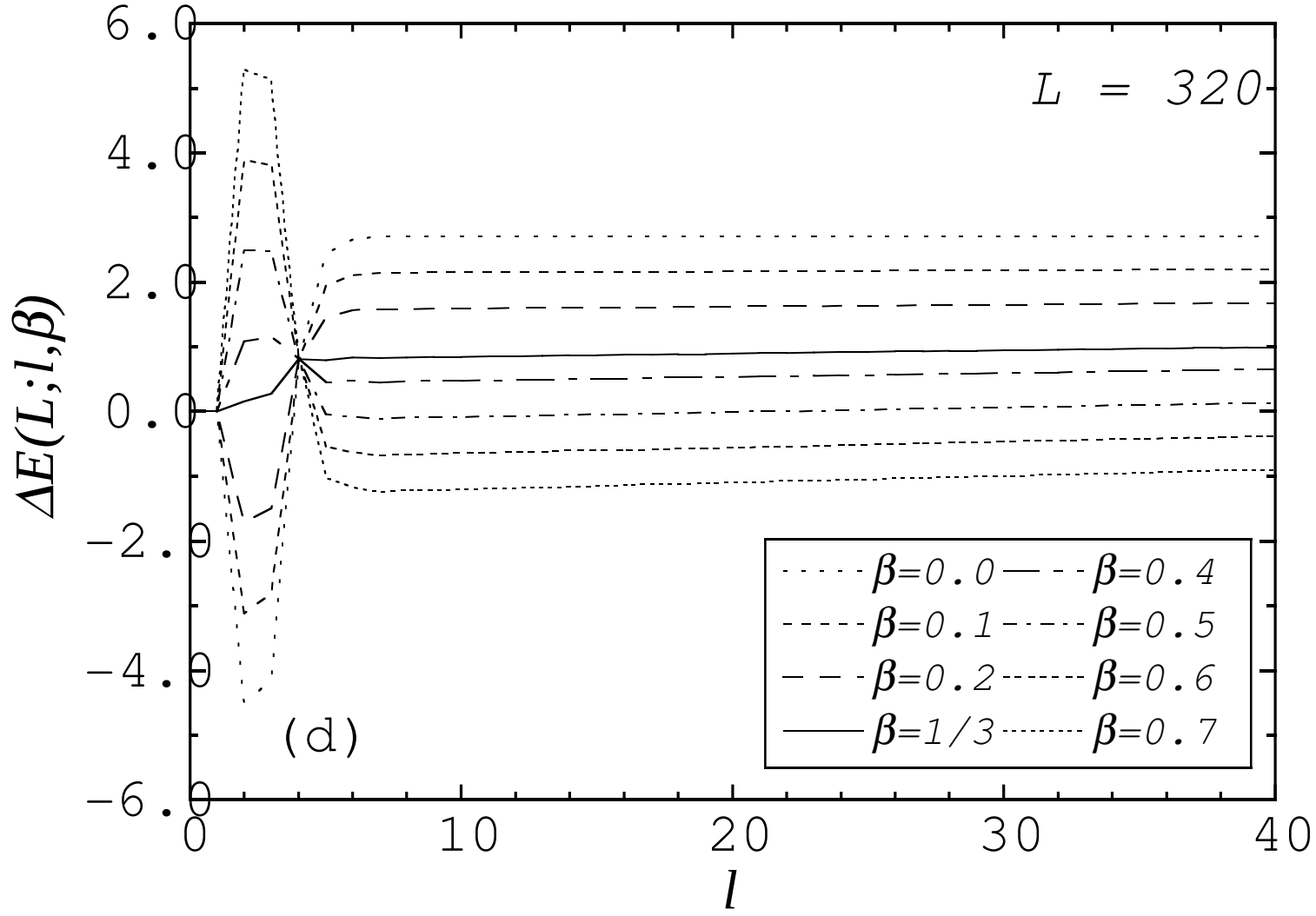
6.0
4.0
2.0
0.0
−2.0
−4.0
−6.0
0
10
20
30
40
l
ΔE(L;l,β)
L = 320
(d)
β=0.0
β=0.1
β=0.2
β=1/3
β=0.4
β=0.5
β=0.6
β=0.7

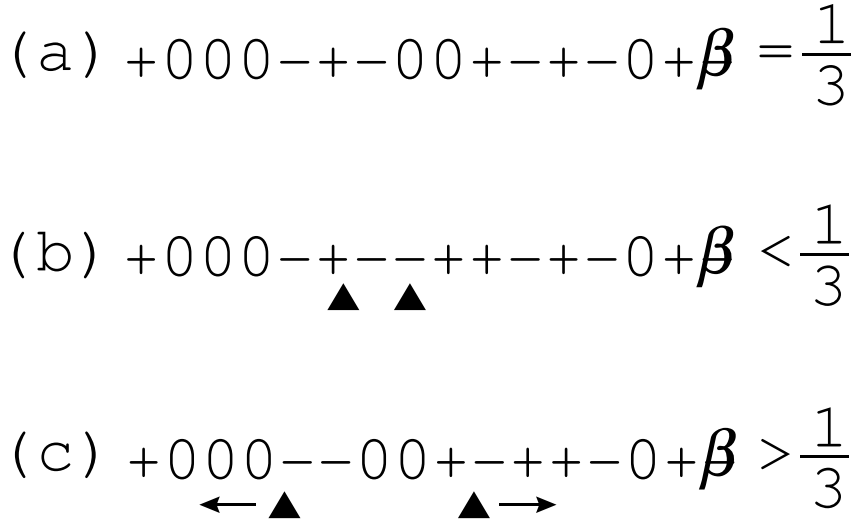

Fig.5